

Supporting Information for Publication

Vacancy Fused Multiple Layers of Copper Sulfoselenide Superstructures: A Propitious HER Electrocatalyst in Acidic Medium

Sangeetha Kumaravel,^{†‡} Dhirendra Kumar,[§] Selvasundarasekar Sam Sankar,^{†‡} Arun Karmakar ^{†‡} Ragunath Madhu,^{†‡} Krishnendu Bera,^{†‡} Hariharan N Dhandapani,^{†‡} Sreenivasan Nagappan,^{†‡} Sudip Chakraborty,^{§,*} and Subrata Kundu^{†‡*}

[†] *Electrochemical Process Engineering (EPE) Division, CSIR-Central Electrochemical Research Institute (CECRI), Karaikudi-630003, Tamil Nadu, India.*

[‡] *Academy of Scientific and Innovative Research (AcSIR), Ghaziabad-201002, India.*

[§] *Materials Theory for Energy Scavenging (MATES) Lab, Harish-Chandra Research Institute, A CI of Homi Bhabha National Institute, Chhatnag Road, Jhansi, Prayagraj-211019, India.*

*To whom correspondence should be addressed, *E-mail:* skundu@cecri.res.in; kundu.subrata@gmail.com and sudipchakraborty@hri.res.in; Tel: +91 4565-241487.

This file contains pages from S1 to S27, where the detailed, reagents and instruments used in the study, figures and Tables corresponding to Cu₂S-Se has been given.

Number of Pages: 27

Number of Figures: 18

Number of Tables: 01

Figures and Tables	Subject of the Figures	Page no.
S1	Synthesis scheme involves the formation of Cu₂S and Cu₂SSe by following hydrothermal methods	S7
S1	Stacked XRD pattern of hydrothermally prepared Cu₂S@Cu foam and Cu₂S-Se@Cu foam and Zoomed XRD pattern of the same indicating the shift after selenization	S8
S2	Low and high magnified FE-SEM images of hydrothermally prepared Cu₂S nano-needles and Low and high magnified images of layered Cu₂S-Se-Hyd sample	S9
S3	The HR-TEM image of layered structure of Cu₂S-Se-Wet	S10
S4	EDS analysis of the Wet-chemically prepare samples such as Cu₂S-Hyd and Cu₂S-Se-Hyd	S11
S5	EDS analysis of the hydrothermally prepare samples such as Cu₂S-Hyd and Cu₂S-Se-Hyd	S12
S6	HR-TEM image of layered Cu₂S-Se-Wet and mixed HAADF elemental mapping of Cu₂S-Se-Wet	S13
S7	XPS spectra of Cu₂S-Se-Hyd; high-resolution images of Cu 2p; O 1s; S 2p and Se 3d	S14
S8	Bar diagram for the overpotential comparison before and after cycling study	S15
S9	Post EIS study for Cu₂S-Wet, Cu₂S-Hyd, Cu₂S-Se-Wet and Cu₂S-Se-Hyd	S16

S10	Mass activity calculated at different current density and Turnover frequency (TOF) calculated at 300 mV overpotential	S17
S11	Faradaic efficiency calculated for Cu₂S-Se-Wet and plot compared with theoretical calculation Vs time.	S18
S12	The potential Vs current density plot for all the four catalyst	S19
S13	Total pDOS of Cu(111) plane	S20
S14	Total pDOS of Cu₂S-Se system	S21
S15	Low and High magnified post SEM images of layered structure of Cu₂S-Se-Wet catalyst	S22
S16	Post HR-TEM image of layered Cu₂S-Se-Wet and mixed post HAADF elemental mapping of Cu₂S-Se-Wet	S23
S17	Post EDS analysis of the wet-chemical sample Cu₂S-Se-Wet	S24
S18	Post XPS spectra of Cu₂S-Se-Wet; high-resolution images of Cu 2p; O 1s; S 2p and Se 3d	S25
Table S1	Comparison of HER performance of Cu₂S-Se-Wet catalyst with other transition metal based catalyst in terms of methodology, overpotential, Tafel slope, binder and substrate	S26

Instruments used in the studies

Before and after selenization, the four set of catalyst such as CuS-Wet, CuS-Hyd, CuS-Se-Wet and CuS-Se-Hyd was characterized using the techniques such as XRD, FE-SEM, HR-TEM, EDS, HAADF, EPR and XPS analysis. The X-ray diffraction (XRD) analysis was carried using a PAN analytical Advanced Bragg-Brentano X-ray powder diffractometer (XRD) with Cu K_{α} radiation ($\lambda = 0.154178$ nm) with a scanning rate of 0.020 s⁻¹ in the 2θ range 10 - 80° . The morphological studies and the HAADF color mapping of both the electrocatalyst was carried in HR-TEM, (TecnaiTM G2TF20) working at an accelerating voltage of 200 kV. The Energy Dispersive X-ray Spectroscopy (EDS) analysis was done with the HR-TEM with a separate EDS detector (INCA) connected to that instrument. The X-ray photoelectron spectroscopic (XPS) analysis was done to check the state of elements present in the outermost part of materials and analyzed by using Theta Probe AR-XPS System, Thermo Fisher Scientific (U.K). The Electron ParaMagnetic Resonance (EPR) Spectroscopy, was performed in EMX Plus X Band with the software of Bruker WIN EPR Acquisition and Processing and the source used are microwaves. Further, the Field Emission Scanning Electron Microscope (FE-SEM) analysis was performed using SUPRA 55VP, Gemini Column with air lock system (Carl Zeiss, Germany). The entire HER study was carried out using Aut-M204 instrument. SCE (reference electrodes) was purchased from the Aut-M204 auto-lab instrument and the Pt (counter electrode) were purchased from Alfa- Aesar.

Materials used and sample preparation for various characterizations

For the preparation of Cu_2S and $\text{Cu}_2\text{S-Se}$, the precursor used are sodium sulfide (Na_2S) (98%), selenium (Se) metal powder (99.99%) and Sodium borohydride (NaBH_4) (98%) was purchased from Sigma-Aldrich. Also, the Cu foam was procured from Alfa-aesar. The deionized water (DI) has been used for the complete study. After the formation of the catalyst, the various characterization studies were carried out such as XRD, FE-SEM, HR-TEM, EDS, HAADF, EPR and XPS analysis. For XRD, FE-SEM, EPR, and XPS analysis, the as prepared electrodes were directly taken for the studies. For HR-TEM, EDS and HAADF colour mapping, the catalyst such as Cu_2S and $\text{Cu}_2\text{S-Se}$ developed over Cu foam was sonicated in DI water for 1 hour and the solution was straight away dropped over the copper coated carbon grid followed by steady evaporation at room temperature. The same has been studied for EDS and HAADF colour mapping with the separate detector system with the HR-TEM instrument.

Mass activity calculation

Current observed in particular potential for the for Cu₂S-Wet, Cu₂S-Hyd, Cu₂S-Se-Wet and Cu₂S-Se-Hyd catalysts

Mass loading calculated for **Cu₂S-Wet and Cu₂S-Hyd** = 0.1 mg cm⁻²

Mass loading calculated for **Cu₂S-Se-Wet and Cu₂S-Hyd** = 0.2 mg cm⁻²

Fixed Overpotential (V)	Current density of Cu₂S-Wet in mA cm⁻²	Current density of Cu₂S-Hyd in mA cm⁻²	Current density of Cu₂S-Se-Wet in mA cm⁻²	Current density of Cu₂S-Se-Hyd in mA cm⁻²
-0.3	-3.94	-3.96	-64.657	-20.147
-0.35	-8.0	-8.0	-198.189	-60.611
-0.4	-37.551	-25.64	-534.352	-145.897

Mass activity is calculated using the formulae,

$$\text{Mass activity} = \text{Current density/Loading of a catalyst}$$

Hence, the mass activity calculated all the four catalyst at high current density **-0.4 V**,

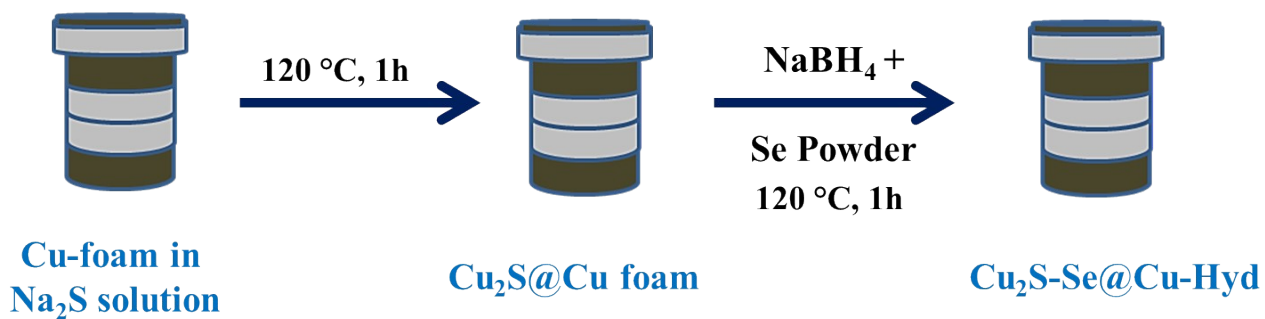
Mass activity calculated = $-37.551/0.1 = 375.51$ mA/mg cm⁻² for **Cu₂S-Wet**

Mass activity calculated = $-25.64/0.1 = 25.64$ mA/mg cm⁻² for **Cu₂S-Hyd**

Mass activity calculated = $-534.352/0.2 = 2674.76$ mA/mg cm⁻² for **Cu₂S-Se-Wet**

Mass activity calculated = $-145.897/0.2 = 734.485$ mA/mg cm⁻² for **Cu₂S-Se-Hyd**

Hydrothermal method



Scheme S1. Synthesis scheme involves the formation of Cu_2S and $\text{Cu}_2\text{S-Se}$ by following hydrothermal methods.

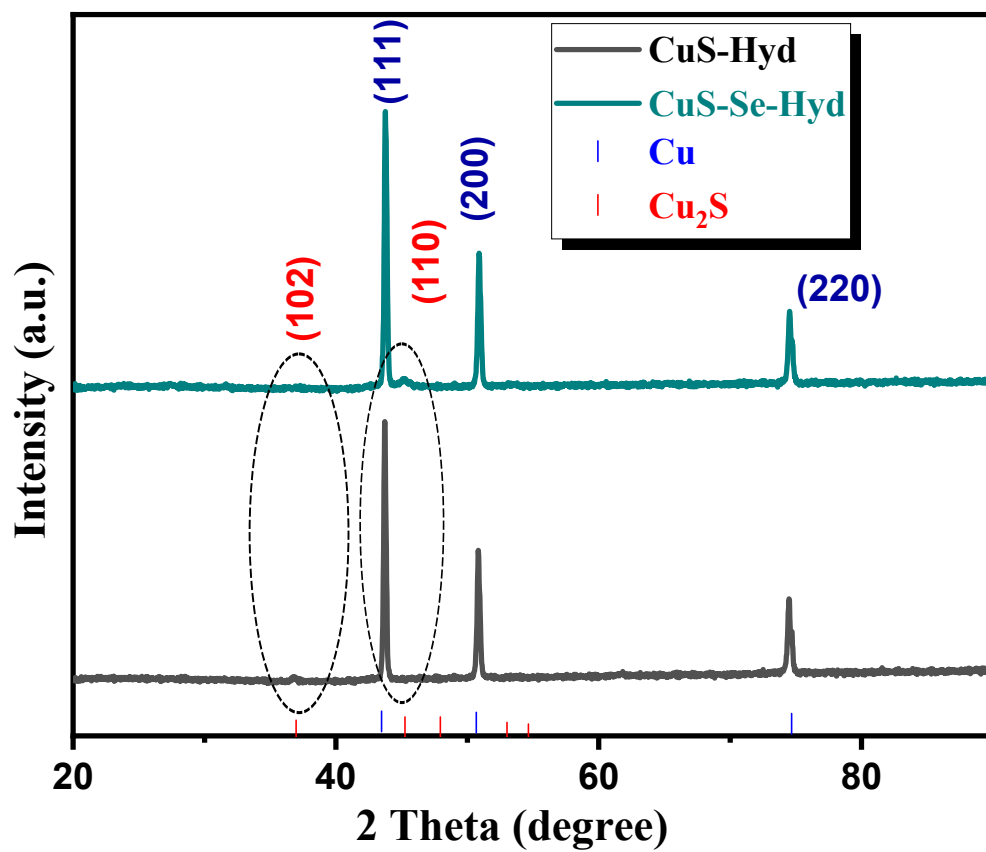


Figure S1. Stacked XRD pattern of hydrothermally prepared Cu₂S@Cu foam and Cu₂S-Se@Cu foam and (b) Zoomed XRD pattern of the same indicating the shift after selenization.

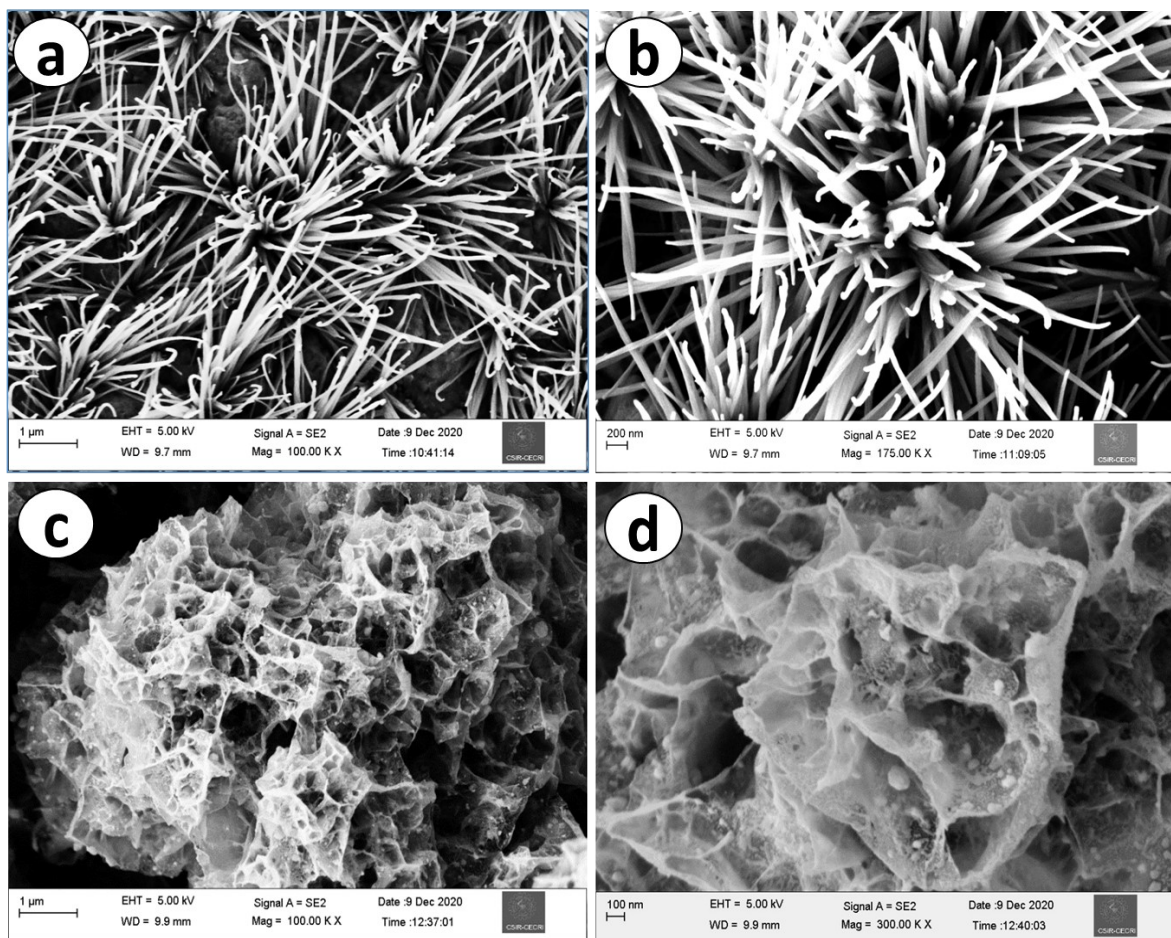


Figure S2. (a and b) Low and high magnified FE-SEM images of hydrothermally prepared Cu_2S nano-needles and (c and d) Low and high magnified images of layered Cu_2S -Se-Hyd sample.

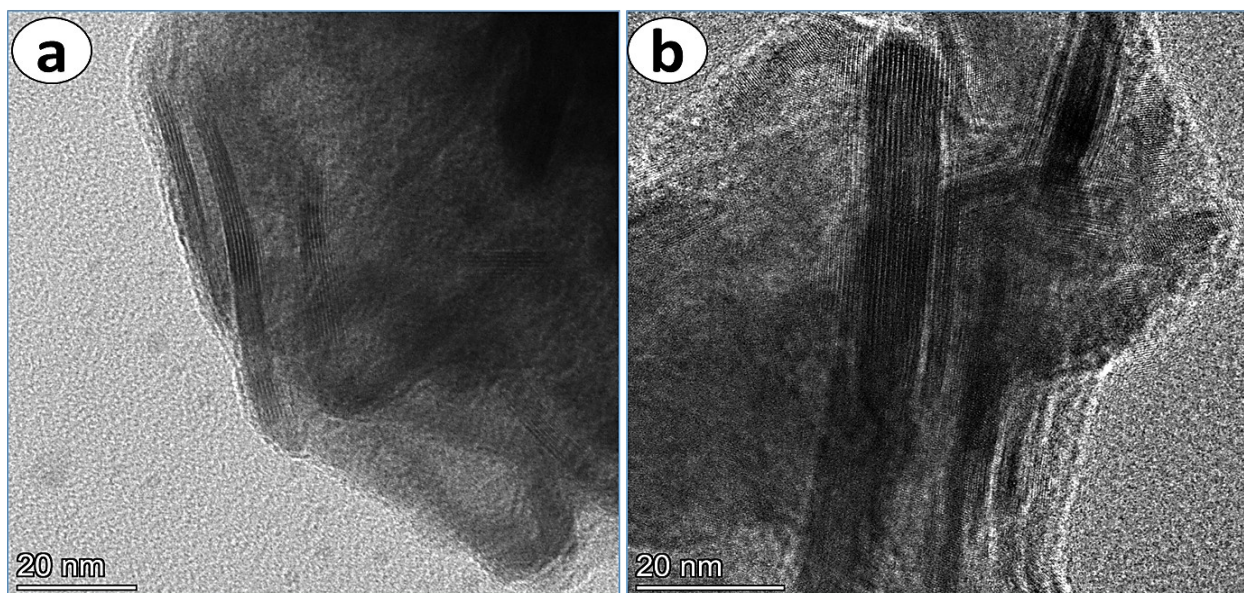


Figure S3. The HR-TEM image of layered structure of $\text{Cu}_2\text{S-Se-Wet}$.

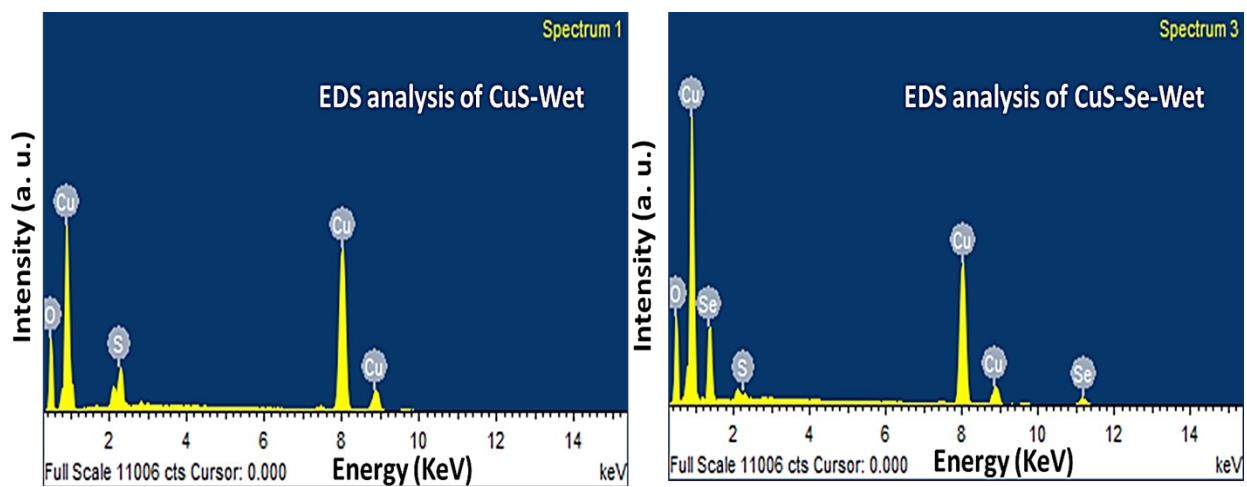


Figure S4. EDS analysis of the wet-chemically prepared samples such as $\text{Cu}_2\text{S-Wet}$ and $\text{Cu}_2\text{S-Se-Wet}$.

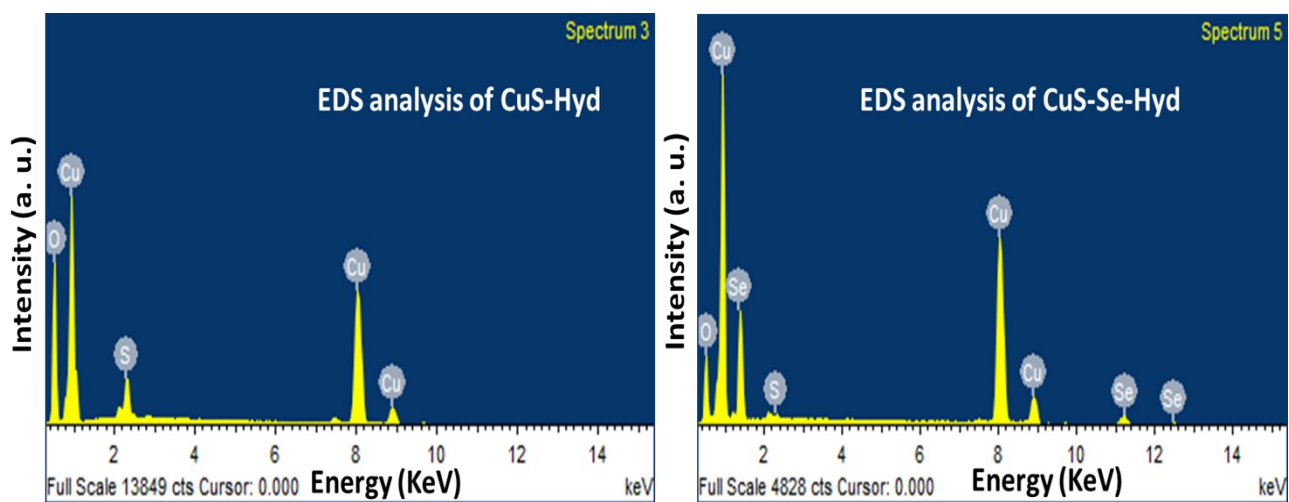


Figure S5. EDS analysis of the hydrothermally prepare samples such as $\text{Cu}_2\text{S-Hyd}$ and $\text{Cu}_2\text{S-Se-Hyd}$.

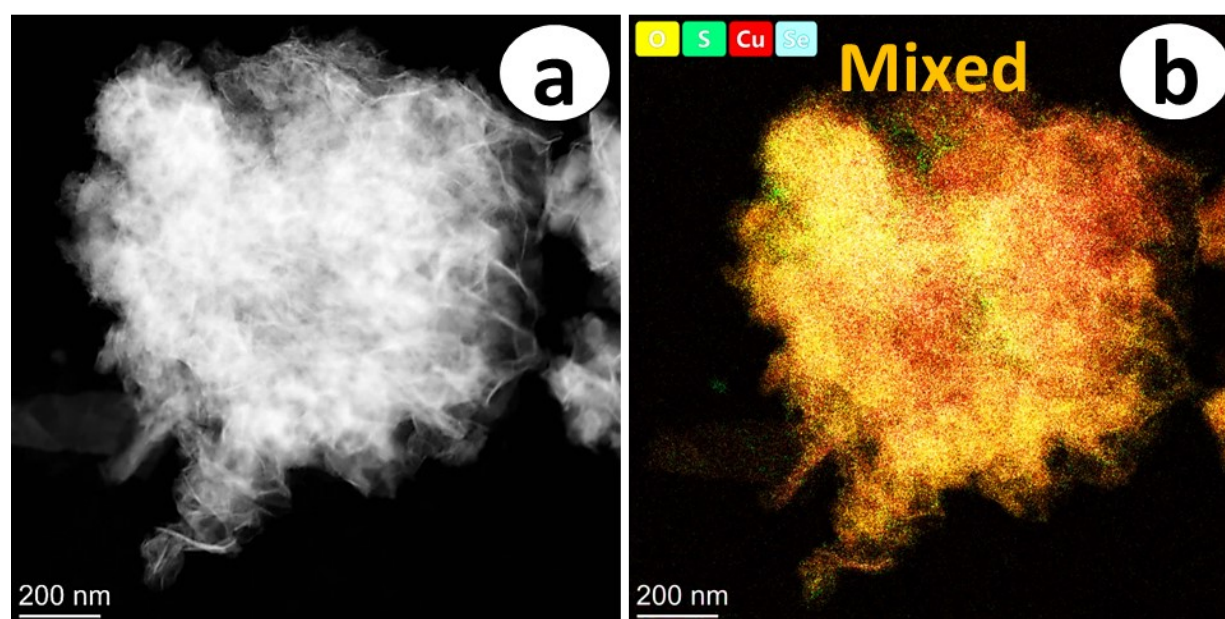


Figure S6. (a) HR-TEM image of layered $\text{Cu}_2\text{S-Se-Wet}$ and (b) mixed HAADF elemental mapping of $\text{Cu}_2\text{S-Se-Wet}$.

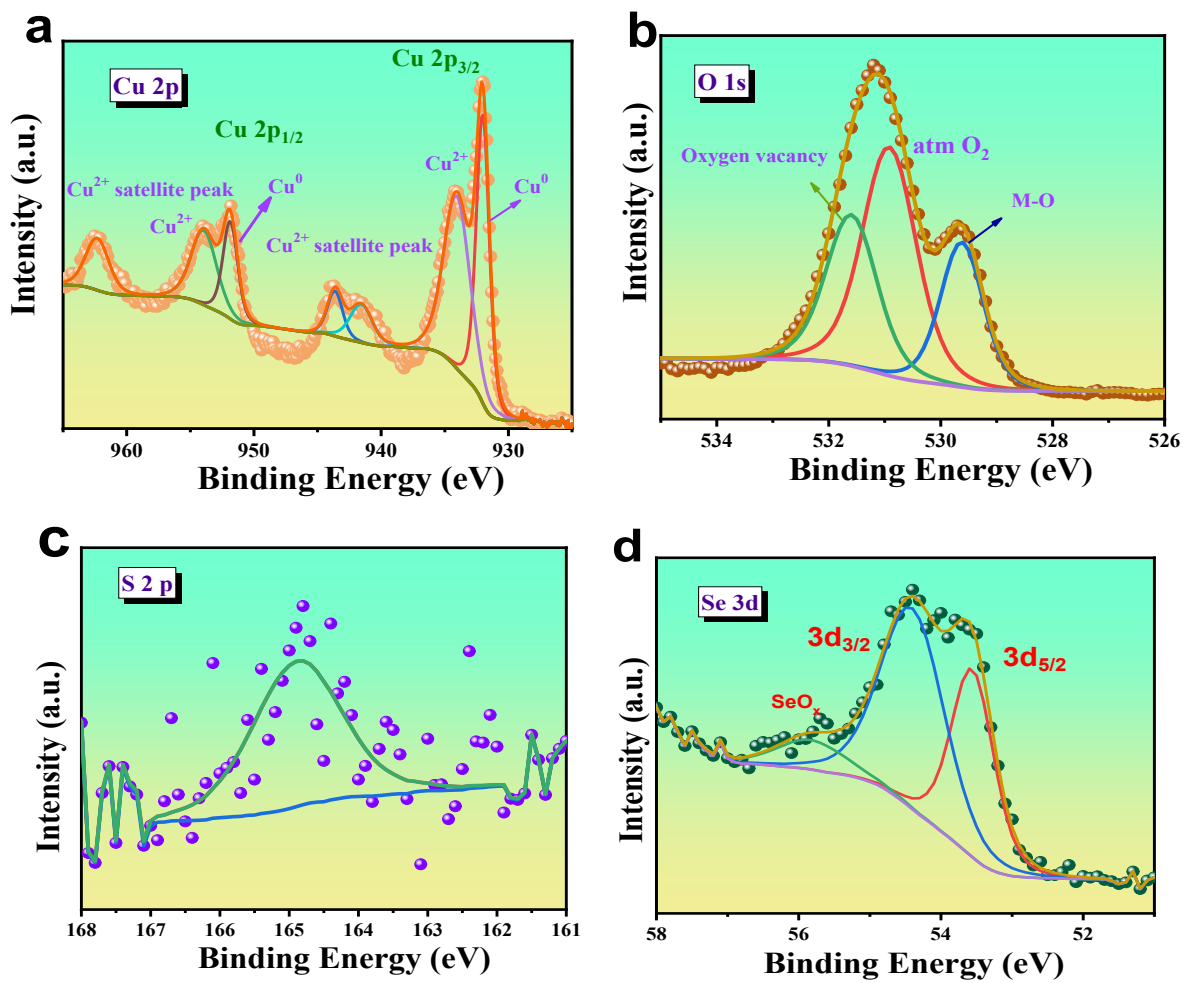


Figure S7. XPS spectra of Cu₂S-Se-Hyd; high-resolution images of (a) Cu 2p; (b) O 1s; (c) S 2p and (d) Se 3d.

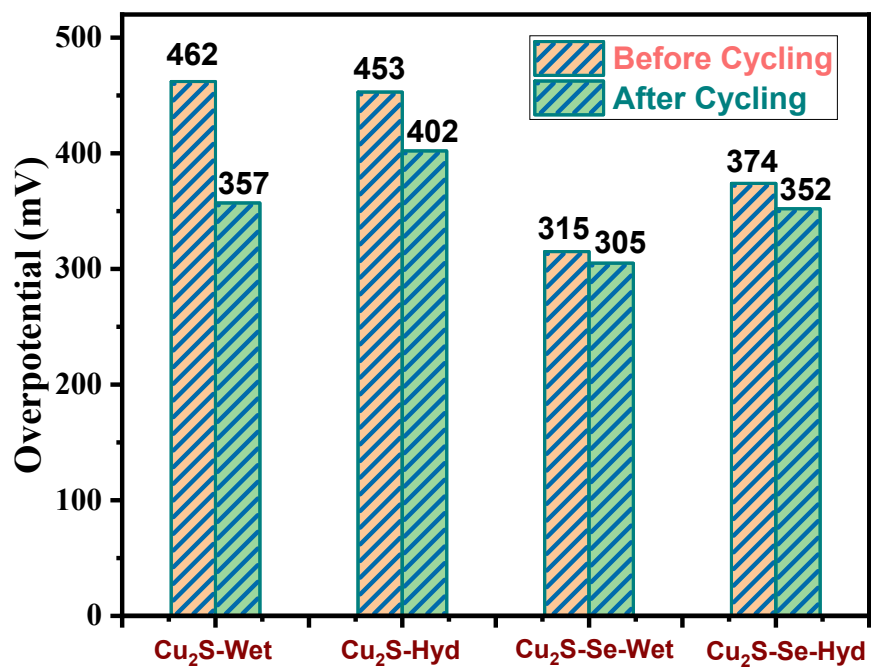


Figure S8. Bar diagram for the overpotential comparison before and after cycling study.

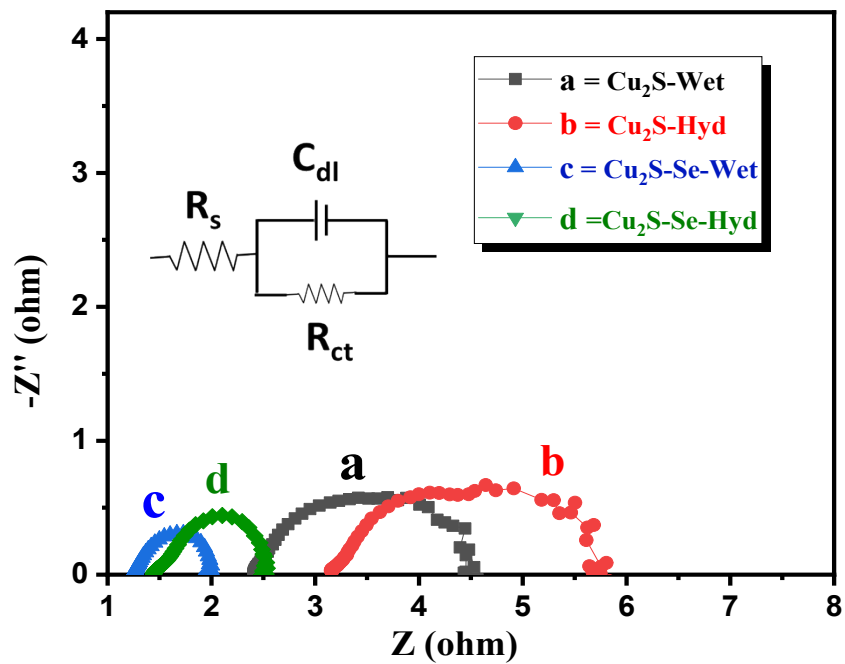


Figure S9. Post EIS study for Cu₂S-Wet, Cu₂S-Hyd, Cu₂S-Se-Wet and Cu₂S-Se-Hyd.

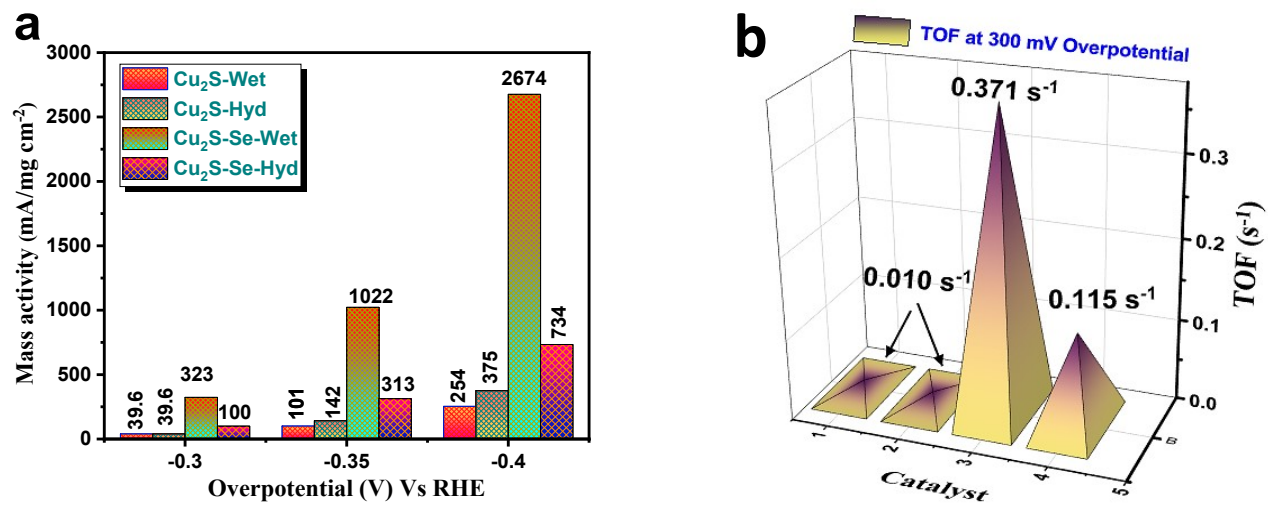


Figure S10. (a) Mass activity calculated at different current density and (b) Turnover frequency (TOF) calculated at 300 mV overpotential.

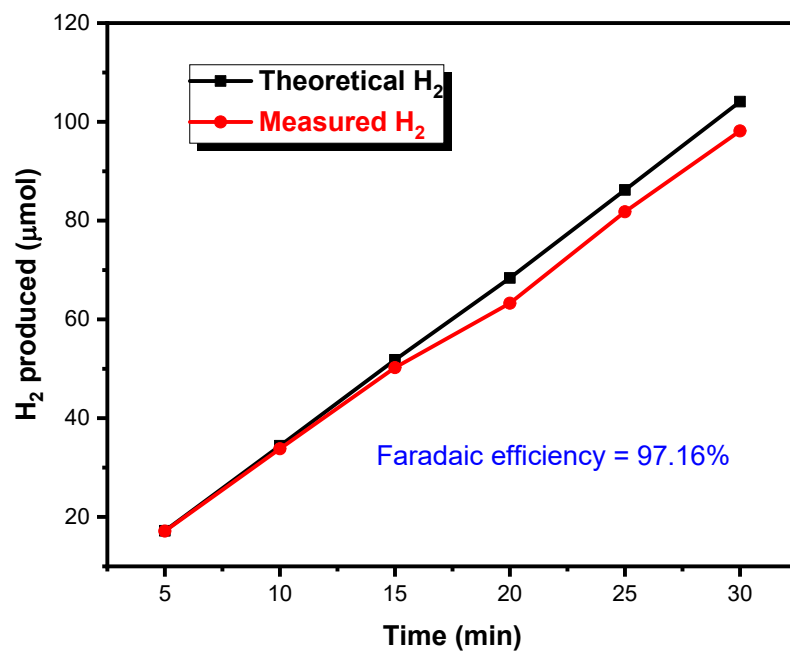


Figure S11. Faradaic efficiency calculated for Cu₂S-Se-Wet and plot compared with theoretical calculation Vs time.

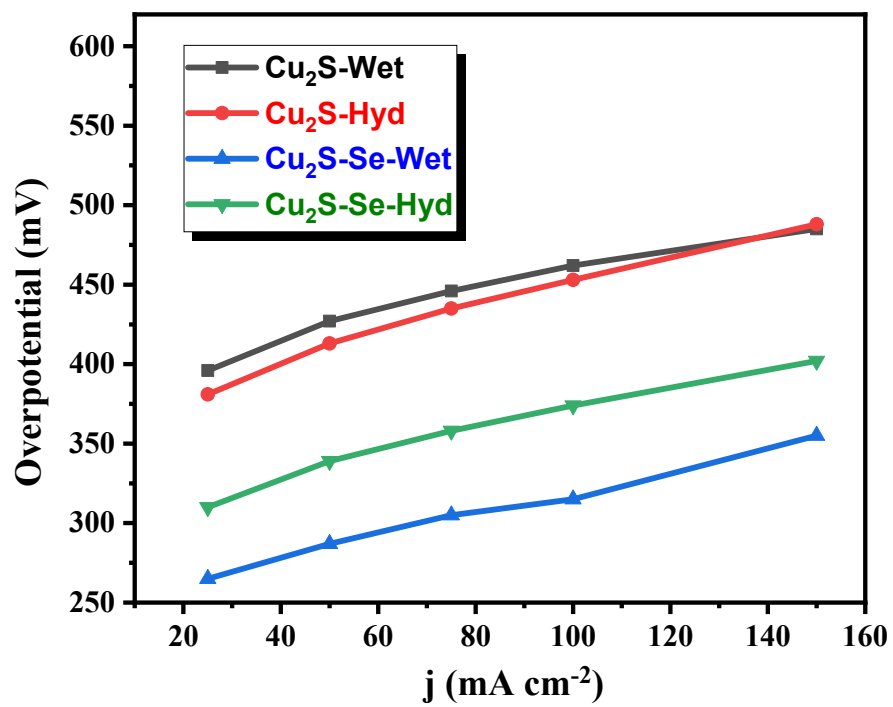


Figure S12. The potential Vs current density plot for all the four catalyst.

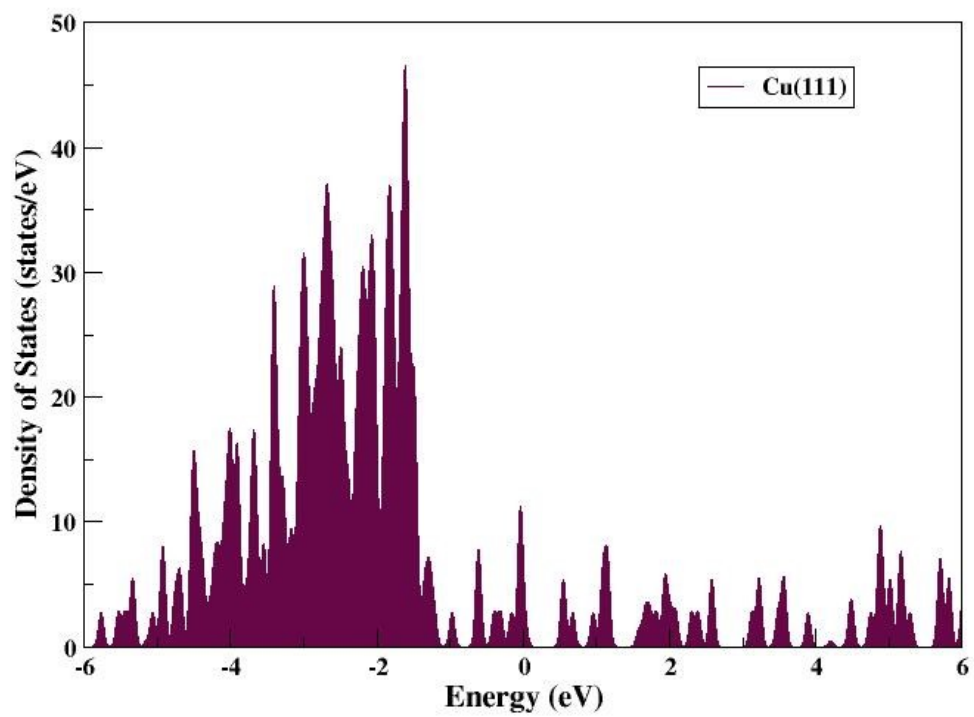


Figure S13. Total pDOS of Cu(111) plane.

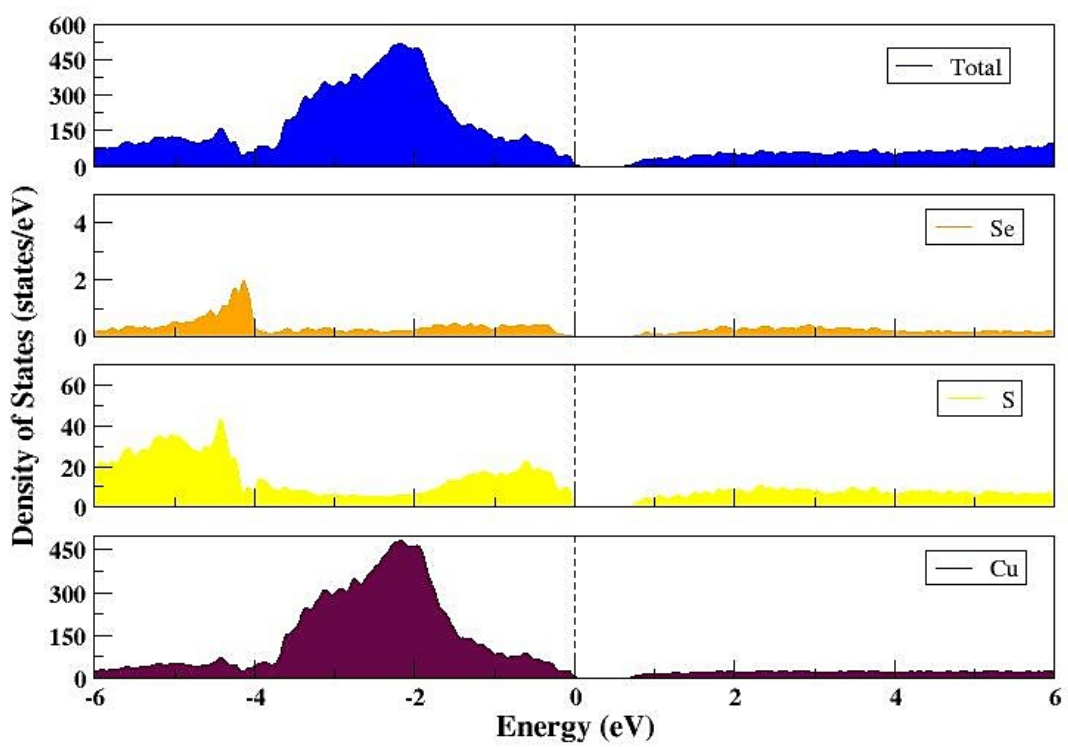


Figure S14. Total pDOS of $\text{Cu}_2\text{S-Se}$ system.

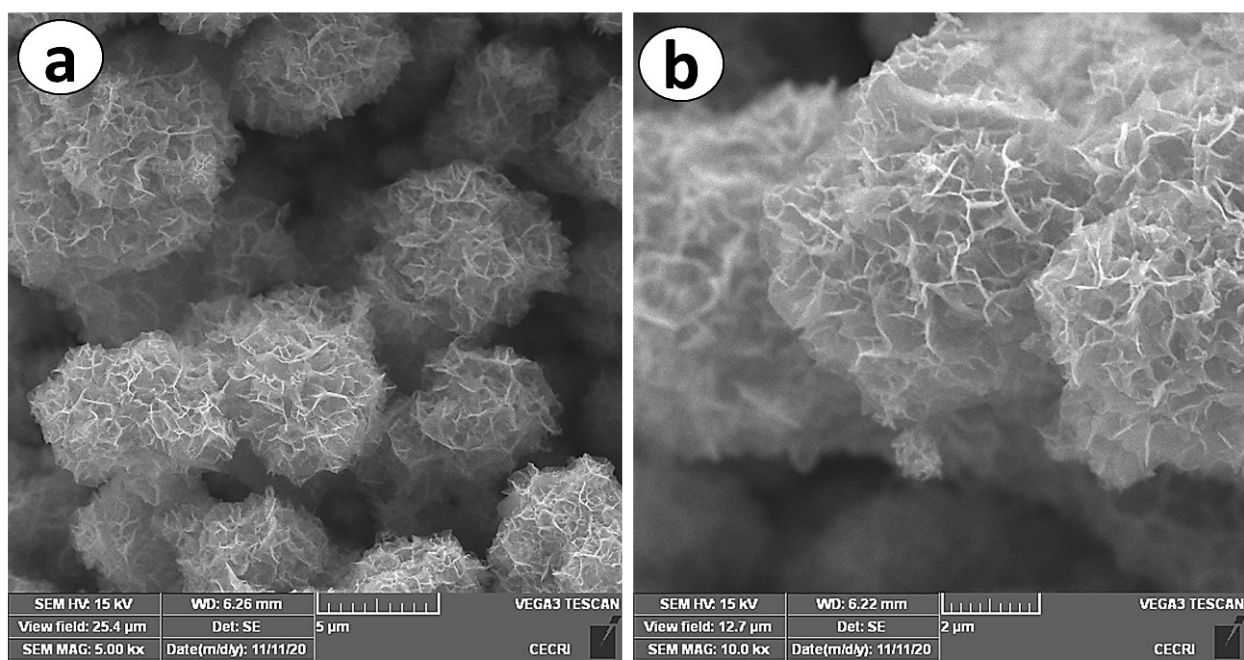


Figure S15. Low and High magnified post SEM images of layered structure of $\text{Cu}_2\text{S-Se-Wet}$ catalyst.

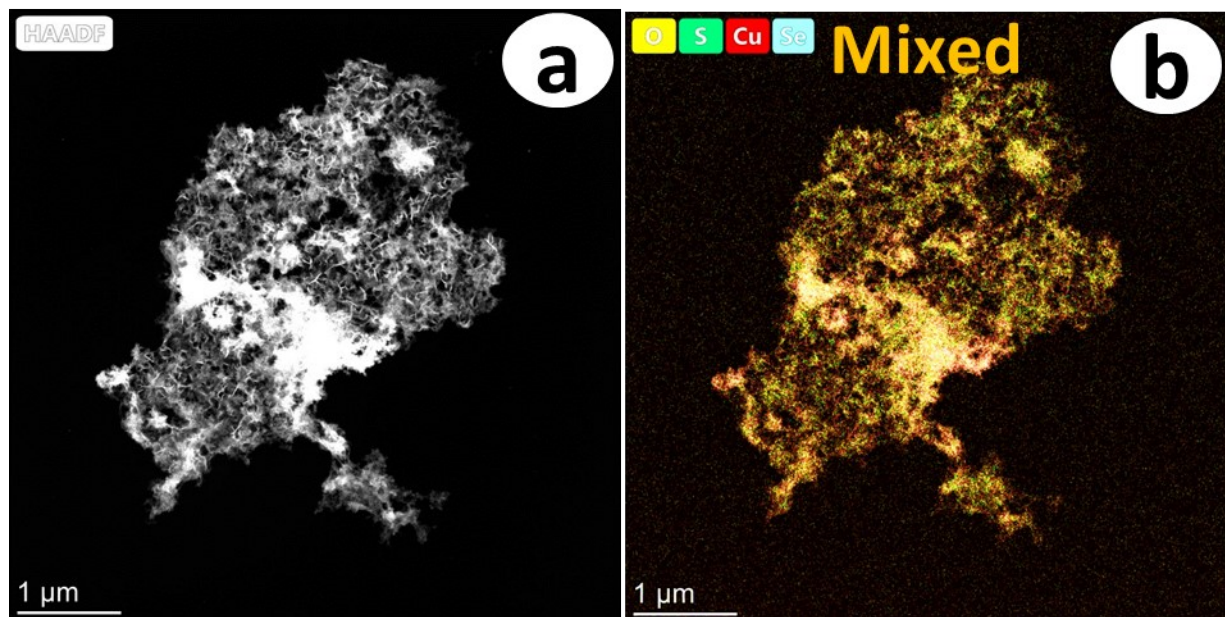


Figure S16. (a) Post HR-TEM image of layered $\text{Cu}_2\text{S-Se-Wet}$. (b) mixed post HAADF elemental mapping of $\text{Cu}_2\text{S-Se-Wet}$.

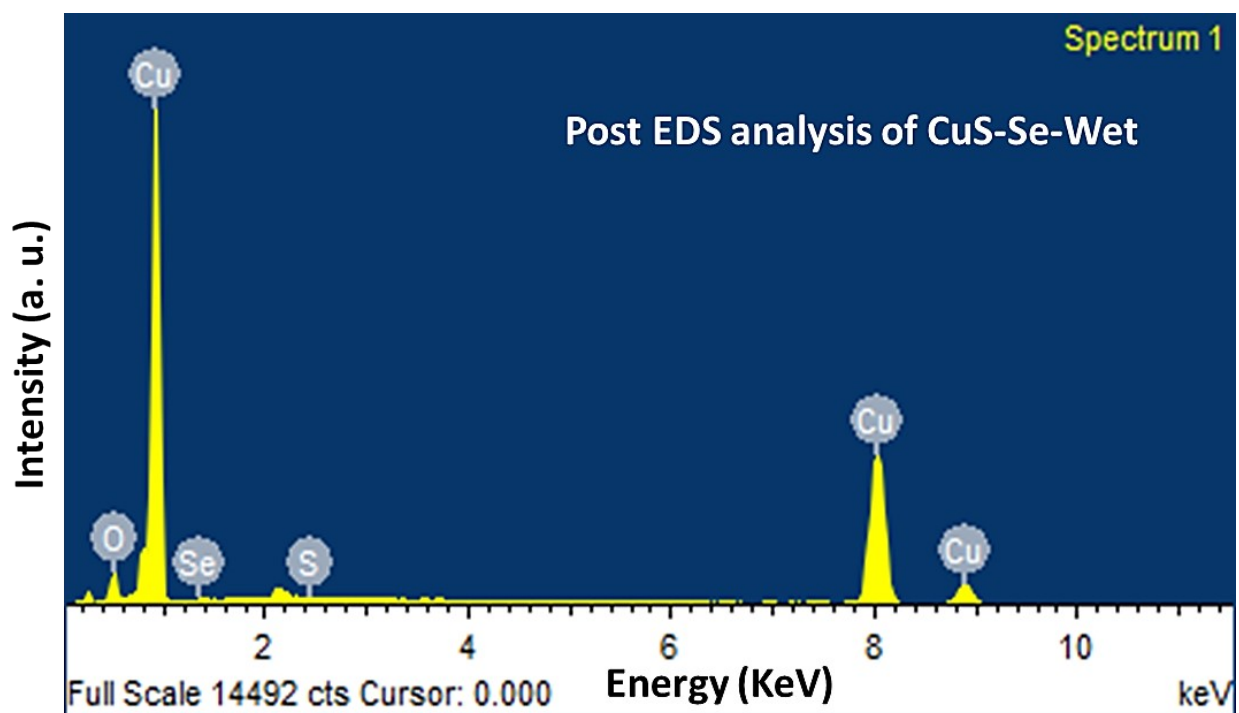


Figure S17. Post EDS analysis of the wet-chemical sample $\text{Cu}_2\text{S-Se-Wet}$.

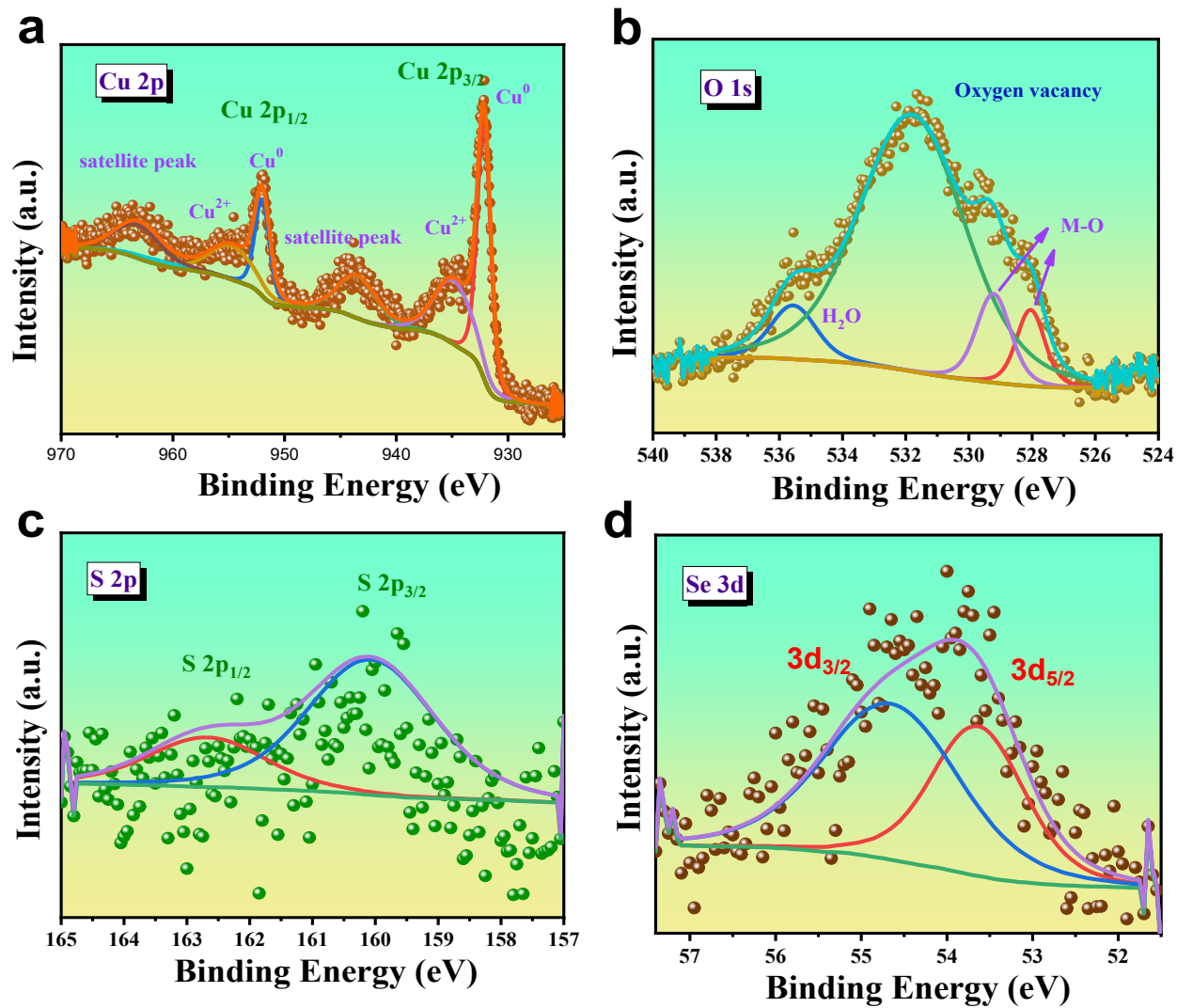


Figure S18. Post XPS spectra of Cu₂S-Se-Wet; high-resolution images of (a) Cu 2p; (b) O 1s; (c) S 2p and (d) Se 3d.

Table S1. Comparison of HER performance of Cu₂S-Se-Wet catalyst with other transition metal based catalyst in terms of methodology, overpotential, Tafel slope, binder and substrate.

Catalysts	Synthesis methods	Overpotential @ 10 mA cm⁻²	Tafel (mV/dec)	Binder	Substrate	Reference
NiCo ₂ S ₄	Hydrothermal	345 mV	60	Nafion	Glassy Carbon	1
Cu ₂ S	Hydrothermal	312 mV	49.79	Nafion	Graphite rod	2
NiS _x	Atomic layer deposition	440 mV	62	-	FTO	3
Ni-WSe ₂	Wet chemical synthesis	259 mV	86	Nafion	Glassy Carbon	4
MoS ₂ Nanosheet arrays	Physical vapour deposition	224 mV	58	-	Carbon Cloth	5
NiS ₂ /GS	Chemical growth	240 mV	41	-	Graphite	6
CoS ₂	Hydrothermal	254 mV	90	Nafion	Glassy Carbon	7
CoSe ₂	Hydrothermal	125 mV	45	-	Ti foil	8
α -NiS	Topotactic conversion	105 mV	40	-	Glassy Carbon	9
NiSe ₂	Solvothermal	147 mV	63	NMP	Carbon paper	10
Cu ₂ S-Se-Wet	Wet-chemical	230 mV	97	-	Cu Foam	This work

References

- 1 U. Aftab, A. Tahira, R. Mazzaro, V. Morandi, M. Ishaq Abro, M. M. Baloch, C. Yu and Z. H. Ibupoto, *RSC Adv.*, 2020, **10**, 22196–22203.
- 2 K. S. Bhat and H. S. Nagaraja, *J. Sci. Adv. Mater. Devices*, 2020, **5**, 361–367.
- 3 Y. Çimen, A. W. Peters, J. R. Avila, W. L. Hoffeditz, S. Goswami, O. K. Farha and J. T. Hupp, *Langmuir*, 2016, **32**, 12005–12012.
- 4 S. R. Kadam, A. N. Enyashin, L. Houben, R. Bar-Ziv and M. Bar-Sadan, *J. Mater. Chem. A*, 2020, **8**, 1403–1416.
- 5 X. Zhang, Y. Zhang, B. Bin Yu, X. L. Yin, W. J. Jiang, Y. Jiang, J. S. Hu and L. J. Wan, *J. Mater. Chem. A*, 2015, **3**, 19277–19281.
- 6 X. Wu, B. Yang, Z. Li, L. Lei and X. Zhang, *RSC Adv.*, 2015, **5**, 32976–32982.
- 7 R. A. Senthil, J. Pan, Y. Wang, S. Osman, T. R. Kumar and Y. Sun, *Ionics (Kiel)*, 2020, **26**, 6265–6275.
- 8 C. P. Lee, W. F. Chen, T. Billo, Y. G. Lin, F. Y. Fu, S. Samireddi, C. H. Lee, J. S. Hwang, K. H. Chen and L. C. Chen, *J. Mater. Chem. A*, 2016, **4**, 4553–4561.
- 9 X. Long, G. Li, Z. Wang, H. Zhu, T. Zhang, S. Xiao, W. Guo and S. Yang, *J. Am. Chem. Soc.*, 2015, **137**, 11900–11903.
- 10 Z. Li, X. Ma, L. Wu, H. Ye, L. Li, S. Lin, X. Zhang, Z. Shao, Y. Yang and H. Gao, *RSC Adv.*, 2021, **11**, 6842–6849.